Available online at www.sciencedirect.com

ScienceDirect

Ceramics International 40 (2014) 1099–1104

CERAMICS INTERNATIONAL

www.elsevier.com/locate/ceramint

A highly conductive and transparent solution processed AZO/MWCNT nanocomposite

Ian Y.Y. Bu[a,*], Matthew T. Cole[b]

[a]Department of Microelectronics Engineering, National Kaohsiung Marine University, 81157 Nanzih District, Kaohsiung City, Taiwan, Republic of China
[b]Department of Engineering, Electrical Engineering Division, University of Cambridge, 9 JJ Thomson Avenue, CB3 0FA Cambridge, United Kingdom

Received 11 June 2013; accepted 28 June 2013
Available online 4 July 2013

Abstract

A solution processed aluminum-doped zinc oxide (AZO)/multi-walled carbon nanotube (MWCNT) nanocomposite thin film has been developed offering simultaneously high optical transparency and low electrical resistivity, with a conductivity figure of merit (σ_{DC}/σ_{opt}) of ~75–better than PEDOT:PSS and many graphene derivatives. The reduction in sheet resistance of thin films of pristine MWCNTs is attributed to an increase in the conduction pathways within the sol–gel derived AZO matrix and reduced inter-MWCNT contact resistance. Films have been extensively characterized by scanning electron microscopy (SEM), energy dispersive spectroscopy (EDS), transmission electron microscopy (TEM), X-ray diffractometry (XRD), photoluminescence (PL), and ultraviolet–visible (UV–vis) spectroscopy.

Keywords: C. Electrical properties; Nano composites; Oxides; Carbon nanotubes; Sol–gel methods

1. Introduction

Carbon nanotubes [1] have attracted considerable interest in the past two decades due to their unique and wide-ranging chemical [2], electrical [3,4] and mechanical properties [5,6]. Though many electronic and photonic devices based on CNTs have been proposed, CNTs have perhaps found their most-widely adopted application in the field of flexible transparent conductive thin films [7,8]. Quasi-metallic multi-walled carbon nanotubes (MWCNTs) [9,10] are formed from incommensurate, concentrically nested, and turbostratically aligned graphene cylinders. They are chemically and mechanically robust and are particularly well suited to functionalization through metal oxide coatings, such as tin oxide, titanium oxide [11], and zinc oxide (ZnO) [12]. Metal-oxide-coated nanotubes possess enhanced opto-electronic properties compared to their as-synthesized, pristine counterparts [13,14] and may become key components in next generation energy storage, display and nanoelectronic devices. Amongst these metal oxides, ZnO [15,16] is possibly the most promising. ZnO is a wide, direct band gap (3.37 eV [17]), large exciton binding energy (60 meV [18]) material that offers solution-based processing at temperatures as low as 90 °C [19,20]. ZnO has also demonstrated significant functionality augmentation in supercapacitors [21], electrochemical sensors [22], and enhanced stability field emitter electron sources [23].

Numerous deposition methods have been adapted to engineer thin films based on ZnO nanoparticles including chemical bath deposition, sol–gel techniques [24,25], chemical vapor deposition [26], sputtering [27], and hydrothermal processing [28–30]. Amongst the most competitive of these techniques is sol–gel processing due to its high material utilization and efficiency, precise composition control, conformal coatings, and low-cost equipment/infrastructure. ZnO nanoparticle coated MWCNTs have been reported elsewhere [31,32] however, to the best of our knowledge, there have been no such reports on aluminum doped zinc oxide (AZO)/MWCNTs hybrid nanocomposites. AZO is commonly used as a transparent conductive oxide layer for Si and group III–IV based solar cells [33]. As such AZO is attractive for transparent thin film as, depending on the Al concentration (0.5–3 at%) and the post-growth annealing conditions, it can

---

*Corresponding author. Tel.: +886 97250 6900; fax: +886 73645589.
E-mail address: ianbu@mail.nkmu.edu.tw (I.Y.Y. Bu).

0272-8842/$ - see front matter
http://dx.doi.org/10.1016/j.ceramint.2013.06.109

possess resistivity several orders of magnitude lower than undoped ZnO [34].

Herein, we report on a spinnable highly conductive transparent AZO/MWCNT nanocomposite fabricated through a facile sol–gel based process. Our hybrids optically and electrically outperform traditional sol-gel synthesized and sputtered AZO thin films as well as chemical vapor deposited pristine MWCNT thin films. The proposed method is fully solution compatible and is widely applicable to a variety of large area applications *via* inexpensive micro-inkjet and nano dip pen techniques [35]. The hybrid AZO/MWCNTs thin films exhibit excellent opto-electronic properties and demonstrate significant potential as transparent conductive electrodes in glass-based solar cells and displays technologies.

2. Experimental

2.1. MWCNT synthesis

MWCNTs were synthesized as described elsewhere [36]. Briefly, catalyst samples were prepared on corning glass by magnetron sputtering 15 nm SiO_2 and 7 nm Fe (100 W) at 3×10^{-4} mbar in Ar. MWCNTs were synthesized by plasma enhanced chemical vapor deposition using a dilution of acetylene in ammonia (C_2H_2: 40 sccm, NH_3: 200 sccm) at 650 °C (100 °C/min). The Ohmically-heated graphite stage was biased to 600 V at a chamber pressure of 3.5 mbar. To remove impurities, as-deposited MWCNTs were treated with H_2SO_4/HNO_3 (3:1), vacuum filtered through a mixed cellulose ester membrane, and washed with deionized water.

2.2. Sol–gel AZO

All analytic grade chemicals were purchased from Sigma Aldrich and were used as received without further purification. Sol–gel precursors were prepared by dissolving 1 M zinc acetate ($Zn(CH_3COO)_2H_2O$) in isopropanol (IPA) with 3 wt% aluminum chloride hexahydrate. Solutions were refluxed for one hour at 70 °C and left to age for at least 24 h. 3 at% (30 ppm) purified MWCNTs were mixed in IPA and the AZO sol–gel, yielding a transparent, light yellow, precipitate-free solution. AZO/MWCNTs solutions were spin coated onto glass substrates, pre-heated to 150 °C and post annealed (at various temperatures) for 10 min. Each cast layer of the hybrid nanocomposite thin film was around 50 ± 5 nm thick. Throughout the precursors were spin coated five times to yield a thickness of ~250 nm. For comparison, AZO thin films were sputtered on glass, as per the conditions described in our previous work [37].

Sample morphology was determined using a FEI Quanta 400F environmental scanning electron microscope (SEM) fitted with an energy dispersive spectrometer (EDS). Crystalline orientations were investigated with a Siemens D5000 X-Ray diffractometer (XRD) using a Cu Kα source ($\lambda = 1.540$ Å). Photoluminescence (PL) studies were performed using a Jasco Model FP-6000 equipped with a 325 nm He–Cd excitation. Electronic transport properties were examined using a Hall system operated in a standard four-probe van der Pauw configuration, at STP.

3. Results and discussion

Fig. 1(**a**) shows an SEM micrograph of the MWCNTs dispersed in acetone and cast on a Si substrate. The MWCNTS were uniformly dispersed and exhibited no visible bundles or aggregations, even in the absence of a surfactant. The MWCNTs were 2–3 μm in length and 50–100 nm in diameter. Fig. 1(**b**) shows SEM micrographs of a typical AZO/MWCNT nanocomposite hybrid deposited at 400 °C. The AZO has a wrinkled/perturbed morphology with small patches scattered on its surface (Fig. 1(**c**)). The films consist of small regions of fiber-like stripes (MWCNTs) embedded within a wrinkled matrix (AZO). The wrinkles were approximately 1 μm in diameter and more than 10 μm in length. Two mechanisms have been proposed to explain wrinkle formation. Kwon [38] argued an increase in volumetric strain, whereas Sherer [39] proposed that a substantial loss of the hydroxyl/ alkoxy groups during sintering induced stress formation. Fig. 1(**d**) shows an AZO/MWCNT film annealed at 550 °C in air. Annealing induced pronounced wrinkling, particularly in films deposited at higher temperatures (550 °C). Bulk shrinkage is most likely caused by rapid solvent evaporation. The derived films evolve from desorption of the hydroxyl groups with subsequent AZO crystallization. Wrinkle formation is beneficial. This wrinkling, pre-stressing phase effectively reduces the intrinsic stress within the film during functional stressing (during operation) making the hybrid nanocomposite well-suited for flexible transparent conductor applications, such as touch screen displays.

Fig. 2(**a**) shows the compositional EDS analysis of the AZO/MWCNT hybrid. Strong Zn (46.6 at%), O (40.2 at%), Al (5.1 at%), and C (8.1 at.%) peaks were detected. The Al content is close to the initial sol-precursor concentration (3 wt%). The spectrometers background C was calibrated to less than 2 at%. All C originates from the MWCNTs. Fig. 2(**b**) shows the XRD patterns of as-prepared composites with and without MWCNTs, in addition to sputtered AZO. The (100), (002), (101), (102), (110), (100), and (103) peaks, ascribed to the ZnO, are indicative of a hexagonal wurtzite structure. Additional peaks at 23.15° and 68.58° account for the MWCNTs graphitic backbone. Sol–gel and sputtered AZO are preferentially orientated in the (002) *c*-axis. It would appear that the (002) peak from the sol–gel derived AZO is sharper than that of the sputtered AZO, suggesting enhanced crystallinity. This is attributed to the fact that the sputtered AZO were deposited at room temperature without post annealing.

The MWCNT additive induces additional intrinsic stresses within the bulk which disrupts *c*-axis orientation, creating alternative ZnO phases. This phenomenon corroborates our SEM findings. The ZnO films become increasingly wrinkled by the addition of an increasing MWCNT content. At the pre-coating stage the MWCNTs and precursor are uniformly mixed. Upon spin coating the MWCNTs remain well dispersed. However, when heated to 150 °C, ZnO starts to crystallize and the MWCNTs agglomerate. Cross-sectional SEM shows that the MWCNTs are not restricted to the film surface but rather exist throughout the bulk.

Fig. 3 shows a low resolution TEM micrographs of a MWCNT bundle coated and intercalated with AZO nanoparticles at different

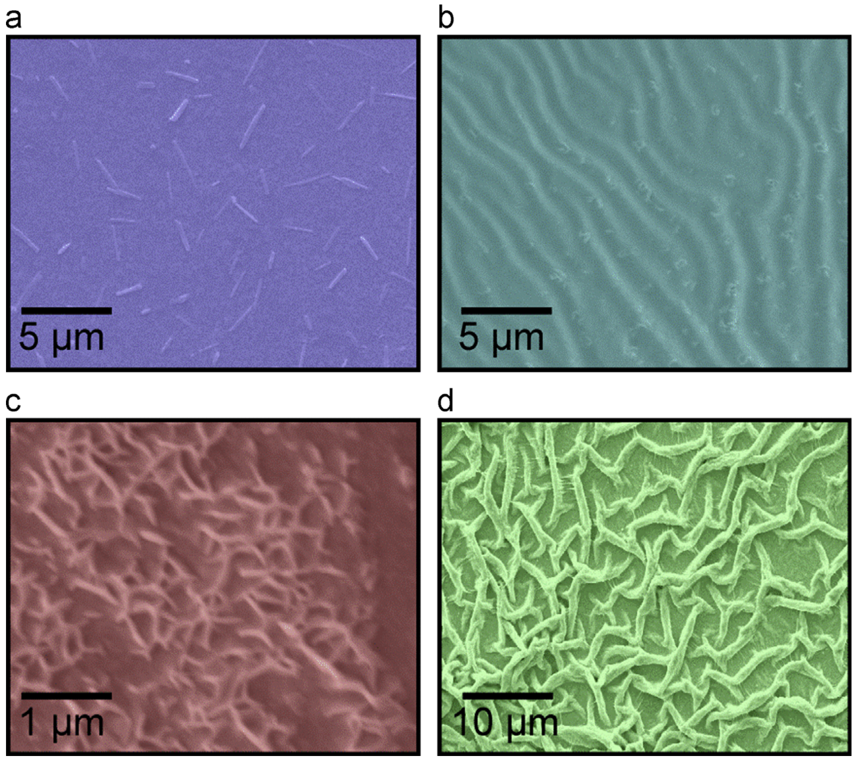

Fig. 1. SEM images of (**a**) uniformly dispersed as-deposited MWCNTs. (**b, c**) a spinned AZO/MWCNT nanocomposite (400 °C) and (**d**) an AZO/MWCNT nanocomposite annealed at 550 °C.

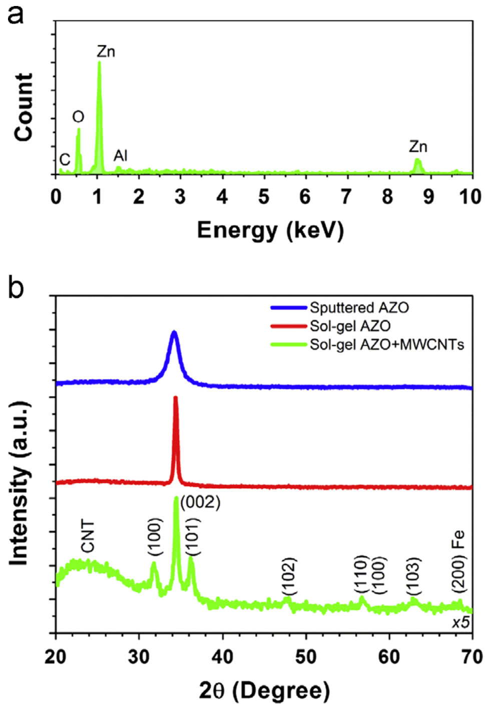

Fig. 2. (**a**) EDS composition of the deposited AZO/MWCNT hybrid nanocomposite. (**b**) XRD patterns of sputtered AZO, sol–gel derived AZO, and the AZO/MWCNT nanocomposite.

resolution. Networks formed from MWCNTs often have a lower conductivity that their constituent MWCNTs [40]. In 1D and 2D nanostructured percolation thin films there is a trade-off between electrical conductivity and optical transparency [41]. High densities of MWCNTs are incorporated to reach acceptably low and technologically relevant electrical resistances. However, as more MWCNTs are introduced the optical transparency degrades due to the increased absorption cross-section. The reduction in resistivity in the AZO/MWCNT nanocomposites originates from reduced contact resistance between MWCNTs and the enhanced interconnectivity between the MWCNTs *via* the AZO interfacial crystallites. The contact resistance between pristine MWCNTs is typically between 23 kΩ and 2.05 MΩ [42,43]. At room temperature, intermolecular tunnel junctions dominate the bulk electron transport. The AZO induces interfacial charge traps, localized states, and local lattice straining. The AZO increases the effective electron transport between the composite MWCNTs due to evanescent-like resonant transmission within the MWCNT/AZO/MWCNT tertiary structure which manifests as an increase in the transmission probability and a consequent reduction in film resistance. Previous studies have shown that MWCNT networks suffer from non-uniform, low conductivity due to voids and discontinuities within the films [40]. The present study resolves this issue by 'filling' these voids with highly conductive AZO. This approach differs from traditional MWCNT networks where optical transparencies are often degraded due the quantity of MWCNTs required to ensure percolation [41,44].

Fig. 4(**a**) shows the optical transparency (UV–vis) of AZO/MWCNT nanocomposites on corning glass substrates, as a function of post-deposition annealing temperature. Processing suitability for glass-based thin film solar cell applications defined an upper practical upper limit of ~600 °C on the annealing temperature. Repeated spin coating and heating/cooling cycles at >600 °C tended to crack the glass substrates. It has also been

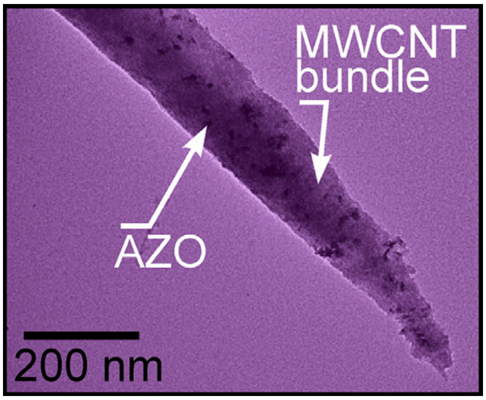

Fig. 3. TEM micrograph of an AZO decorated MWCNT bundle (Scale bar: 200 nm).

shown in previous studies that during sol–gel production of Zn, films must be annealed to at least 450 °C [45] to remove residual organics and induced crystallization. Measurements were taken without subtraction of the glass background to emulate typical photovoltaic cell configurations. All AZO/MWCNT films exhibit excellent transparency ranging from 78% to 88% at 500 nm ($R_s = 30\ \Omega$/sq). Films synthesized at 400 °C were around 80% transparent. Increasing the annealing temperature to 450 °C resulted in a marginal decrease in transparency (78%). Anneal temperatures of 500–550 °C improved the optical transparency to ~88% The lower optical transparency at 450 °C suggests grain disorder, perhaps due to transformation of residual zinc acetate to ZnO. The obtained transparency in our films is close to that of optimized AZO films deposited by RF sputtering at 400 °C [46].

Fig. 4(**b**) shows a PL spectra of pristine AZO and an AZO/MWCNTs nanocomposite. In the case of pristine AZO, the peak at 380 cm^{-1} corresponds to free-exciton recombination band-edge emission [47], whilst the AZO/MWCNT exhibits additional peaks at 435 cm^{-1} and a broad visible emission at 500 cm^{-1}. Well-defined emission indicates high quality AZO and is often associated with [OH^-] ions on the ZnO surface [48]. The peaks at 500 cm^{-1} account for radiative recombination of excitons related to surface defects [49], a consequence of MWCNT incorporation within the sol–gel matrix.

The AZO/MWCNT nanocomposite is *n*-type with a sheet resistance of around 30 Ω/sq. The AZO/MWCNT has a significantly lower sheet resistance than pristine sol–gel (112 Ω/sq) and sputtered (78 Ω/sq) AZO. The resistivity of the composite is towards the lower end of the resitivities reported for optimized AZO (14 Ω/sq – 850 °C for 1 h vacuum sintered films [50]). However, in contrast, our films were synthesized at only 550 °C with a rapid atmospheric hotplate sintering of only 10 min. The inclusion of the MWCNTs increased the carrier density of the AZO matrix markedly, from 7.6×10^{15} to $5.0 \times 10^{17}\ \text{cm}^{-3}$, whilst also increasing the mobility from 16 to 254 cm^2/Vs. The hybrid nanocomposite showed a carrier density some four orders of magnitude greater than sputtered AZO. Incorporation of the MWCNTs in the nanocomposite dramatically lowered the resistivity *via* simple, rapid, low temperature processes enabling the utilization of inexpensive glass substrates whilst simultaneously increasing throughput.

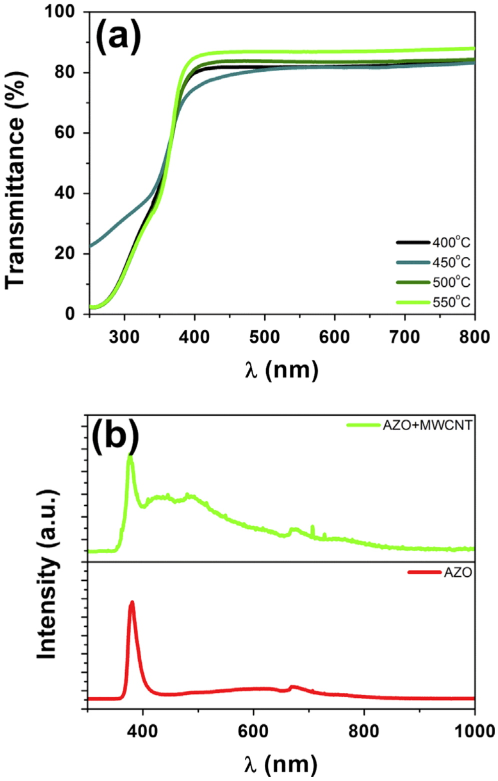

Fig. 4. (**a**) Optical transmittance of the AZO/MWCNT composite annealed at 400–550 °C. (**b**) Photoluminescence spectra of sol–gel derived AZO/MWCNT nanocomposite and pristine sol–gel AZO.

The optical transparency and electronic conductivity of transparent conducting media can be related by $T(\lambda) = (1 + 188.5\sigma_{\text{op}}(\lambda)/R_S\sigma_{\text{DC}})$, where T (λ) is the optical transmission at 550 nm, R_S is the sheet resistivity, σ_{DC} is the DC electrical conductivity, and σ_{opt} is the optical conductivity [40,51,52]. The extracted figure of merit, $\sigma_{\text{DC}}/\sigma_{\text{opt}}$, for the AZO/MWCNT spinnable nanocomposite is around 75, which is higher than chemically exfoliated graphene (1.7 [52,53]) and PEDOT:PSS (40) [54], but lower than Ag nanowire networks (120) and commercially available indium tin oxide (400–800) [51]. For practical applications the accepted figure of merit is ~35 ($T > 90\%$, $Rs < 100\ \Omega$/sq) [54] suggesting that the AZO/MWCNT nanocomposite may find application in touch screens and display applications.

4. Conclusion

A spinnable AZO/MWCNT nanocomposite has been synthesized and considered optically and electrically under different annealing temperatures to study the enhancing effects of a MWCNT additive. The AZO/MWCNT thin films synthesized at temperatures in excess of 500 °C produced highly transparent, low resistive thin films ($\sigma_{\text{DC}}/\sigma_{\text{opt}} = 75$). The AZO/MWCNT nanocomposite is fully solution process-able, highly scalable and utilizes inexpensive equipment demonstrating that earth abundant materials such as Zn, Al, and C can be used to great effect as potential replacements for ubiquitous indium and fluorine doped tin oxides.

Acknowledgments

I.Y.Y. Bu thanks the National Science Council under the Grant NSC 98-2218-E-022 -001 and NSC 99-2628-E-022-001 for financial support. M.T. Cole thanks the Isaac Newton Trust, Trinity College Cambridge University for generous financial support.

References

[1] L. Radushkevich, V. Lukyanovich, About the structure of carbon formed by thermal decomposition of carbon monoxide on iron substrate, Journal of Physical Chemistry (Moscow) 26 (1952) 88–95.

[2] V. Sgobba, D.M. Guldi, Carbon nanotubes electronic/electrochemical properties and application for nanoelectronics and photonics, Chemical Society Reviews 38 (1) (2008) 165–184.

[3] M. Biercuk, S. Ilani, C. Marcus, P. McEuen, Electrical transport in single-wall carbon nanotubes, Carbon Nanotubes (2008) 455–493.

[4] A. Jorio, G. Dresselhaus, M.S. Dresselhaus, Carbon nanotubes: advanced topics in the synthesis, structure, properties and applications, Springer Verlag, Berlin, Germany, 2008.

[5] M. Moniruzzaman, A. Sahin, K.I. Winey, Improved mechanical strength and electrical conductivity of organogels containing carbon nanotubes, Carbon 47 (3) (2009) 645–650.

[6] A.K. Huttel, G.A. Steele, B. Witkamp, M. Poot, L.P. Kouwenhoven, H.S.J. van der Zant, Carbon nanotubes as ultrahigh quality factor mechanical resonators, Nano Letters 9 (7) (2009) 2547–2552.

[7] D. Zhang, K. Ryu, X. Liu, E. Polikarpov, J. Ly, M.E. Tompson, C. Zhou, Transparent, conductive, and flexible carbon nanotube films and their application in organic light-emitting diodes, Nano Letters 6 (9) (2006) 1880–1886.

[8] F.N. Ishikawa, H. Chang, K. Ryu, P. Chen, A. Badmaev, L.Gomez De Arco, G. Shen, C. Zhou, Transparent electronics based on transfer printed aligned carbon nanotubes on rigid and flexible substrates, ACS Nano 3 (1) (2008) 73–79.

[9] P. Avouris, J. Appenzeller, R. Martel, S.J. Wind, Carbon nanotube electronics, Proceedings of the IEEE 91 (11) (2003) 1772–1784.

[10] D. Dragoman, M. Dragoman, Electromagnetic wave propagation in dense carbon nanotube arrays, Journal of Applied Physics 99 (2006) 076106.

[11] Y. Yao, G. Li, S. Ciston, R.M. Lueptow, K.A. Gray, Photoreactive TiO2/carbon nanotube composites: synthesis and reactivity, Environmental Science and Technology 42 (13) (2008) 4952–4957.

[12] H. Kim, H.-H. Park, H. Jeon, H.J. Chang, Y. Chang, H.-H. Park, Incorporation of carbon nanotube into direct-patternable ZnO thin film formed by photochemical solution deposition, Ceramics International 35 (1) (2009) 131–135.

[13] S. Kedem, J. Schmidt, Y. Paz, Y. Cohen, Composite polymer nanofibers with carbon nanotubes and titanium dioxide particles, Langmuir 21 (12) (2005) 5600–5604.

[14] Y. Yang, L. Qu, L. Dai, T.S. Kang, M. Durstock, Electrophoresis coating of titanium dioxide on aligned carbon nanotubes for controlled syntheses of photoelectronic nanomaterials, Advanced Materials 19 (9) (2007) 1239–1243.

[15] J.M. Lee, G.R. Xu, B.K. Kim, H.N. Choi, W.Y. Lee, Amperometric tyrosinase biosensor based on carbon nanotube doped sol gel derived zinc oxide nafion composite films, Electroanalysis 23 (4) (2011) 962–970.

[16] S.C. Gong, J.G. Jang, H.J. Chang, J.-S. Park, The characteristics of organic light emitting diodes with Al doped zinc oxide grown by atomic layer deposition as a transparent conductive anode, Synthetic Metals 161 (9) (2011) 823–827.

[17] Z.L. Wang, Zinc oxide nanostructures: growth, properties and applications, Journal of Physics: Condensed Matter 16 (25) (2004) R829.

[18] M. Hossain, T. Takahashi, Microstructured ZnO photoelectrode grown on the sputter-deposited ZnO passivating-layer for improving the photovoltaic performances, Materials Chemistry and Physic 124 (2-3) (2010) 940–945.

[19] L.E. Greene, M. Law, J. Goldberger, F. Kim, J.C. Johnson, Y. Zhang, R.J. Saykally, P. Yang, Low-temperature wafer-scale production of ZnO nanowire arrays, Angewandte Chemie International Edition 42 (26) (2003) 3031–3034.

[20] F. Fleischhaker, V. Wloka, I. Hennig, ZnO based field-effect transistors (FETs): solution-processable at low temperatures on flexible substrates, Journal of Materials Chemistry 20 (32) (2010) 6622–6625.

[21] Y. Zhang, X. Sun, L. Pan, H. Li, Z. Sun, C. Sun, B.K. Tay, Carbon nanotube–zinc oxide electrode and gel polymer electrolyte for electrochemical supercapacitors, Journal of Alloys and Compounds 480 (2) (2009) L17–L19.

[22] D. Ramírez, R. Segura, H. Gómez, Nanocomposites structures based on the electrochemical assembling of zinc oxide nanorods and carbon nanotubes, Materials Chemistry and Physics (2011).

[23] C. Li, Y. Zhang, M. Mann, P. Hiralal, H. Unalan, W. Lei, B. Wang, D. Chu, D. Pribat, G. Amaratunga, Stable, self-ballasting field emission from zinc oxide nanowires grown on an array of vertically aligned carbon nanofibers, Applied Physics Letters 96 (14) (2010) 143114-143114-143113.

[24] M. Ohyama, H. Kozuka, T. Yoko, Sol gel preparation of transparent and conductive aluminum doped zinc oxide films with highly preferential crystal orientation, Journal of the American Ceramic Society 81 (6) (1998) 1622–1632.

[25] C.L. Tsai, Y.C. Tseng, W.M. Cho, Y.J. Lin, H.C. Chang, Y.H. Chen, C.H. Lin, Effects of ultraviolet treatment on the optical and structural properties of ZnO nanoparticles, Materials Chemistry and Physics (2011).

[26] Y. Wu, Z. Xi, J. Zhang, Q. Zhang, Two types of ZnO-tubular nanostructures fabricated by stepped gas-phase reaction, Materials Chemistry and Physics 110 (2) (2008) 445–448.

[27] Q. Shi, K. Zhou, M. Dai, H. Hou, S. Lin, C. Wei, F. Hu, Room temperature preparation of high performance AZO films by MF sputtering, Ceramics International (2012).

[28] S.-F. Wang, T.-Y. Tseng, Y.-R. Wang, C.-Y. Wang, H.-C. Lu, Effect of ZnO seed layers on the solution chemical growth of ZnO nanorod arrays, Ceramics International 35 (3) (2009) 1255–1260.

[29] S. Sepulveda-Guzman, B. Reeja-Jayan, E. de la Rosa, A. Torres-Castro, V. Gonzalez-Gonzalez, M. Jose-Yacaman, Synthesis of assembled ZnO structures by precipitation method in aqueous media, Materials Chemistry and Physics 115 (1) (2009) 172–178.

[30] L. Zhang, H. Yang, L. Li, Synthesis and characterization of core/shell-type ZnO nanorod/ZnSe nanoparticle composites by a one-step hydrothermal route, Materials Chemistry and Physics 120 (2-3) (2010) 526–531.

[31] Y. Du, C.C. Hao, G. Wang, Preparation of floral-patterned ZnO/MWCNT heterogeneity structure using microwave irradiation heating method, Mater Letters 62 (1) (2008) 30–32.

[32] G. Guo, J. Guo, D. Tao, W. Choy, L. Zhao, W. Qian, Z. Wang, A Simple method to prepare multi-walled carbon nanotube/ZnO nanoparticle composites, Applied Physics A: Materials Science and Processing 89 (2) (2007) 525–528.

[33] J. Nelson, The Physics of Solar Cells, Imperial College Press, London, 2003.

[34] T. Minami, Transparent conducting oxide semiconductors for transparent electrodes, Semiconductor Science and Technology 20 (2005) S35.

[35] K. Salaita, Y. Wang, C.A. Mirkin, Applications of dip-pen nanolithography, Nature Nanotechnology 2 (3) (2007) 145–155.

[36] I.Y.Y. Bu, S.P. Oei, Hydrophobic vertically aligned carbon nanotubes on corning glass for self cleaning applications, Applied Surface Science 256 (22) (2010) 6699–6704.

[37] I.Y.Y. Bu, Facile synthesis of highly oriented p-type aluminum co-doped zinc oxide film with aqua ammonia, Journal of Alloys and Compounds 509 (6) (2011) 2874–2878.

[38] S.J. Kwon, J.H. Park, J.G. Park, Wrinkling of a sol–gel-derived thin film, Physical Review E 71 (1) (2005) 11604.

[39] G.W. Scherer, Sintering of sol–gel films, Journal of Sol–Gel Science and Technology 8 (1) (1997) 353–363.

[40] L. Hu, D. Hecht, G. Grüner, Percolation in transparent and conducting carbon nanotube networks, Nano Letters 4 (12) (2004) 2513–2517.

[41] Z. Wu, Z. Chen, X. Du, J.M. Logan, J. Sippel, M. Nikolou, K. Kamaras, J.R. Reynolds, D.B. Tanner, A.F. Hebard, Transparent, conductive carbon nanotube films, Science 305 (5688) (2004) 1273–1276.

[42] R. Martel, T. Schmidt, H. Shea, T. Hertel, P. Avouris, Single-and multi-wall carbon nanotube field-effect transistors, Applied Physics Letters 73 (17) (1998) 2447–2449.

[43] A. Buldum, J.P. Lu, Contact resistance between carbon nanotubes, Physical Review B 63 (16) (2001) 161403.

[44] M. Kaempgen, G. Duesberg, S. Roth, Transparent carbon nanotube coatings, Applied Surface Science 252 (2) (2005) 425–429.

[45] M. Kamalasanan, S. Chandra, Sol–gel synthesis of ZnO thin films, Thin Solid Films 288 (1) (1996) 112–115.

[46] R. Wen, L. Wang, X. Wang, G.H. Yue, Y. Chen, D.L. Peng, Influence of substrate temperature on mechanical, optical and electrical properties of ZnO: Al films, Journal of Alloys and Compounds 508 (2) (2010) 370–374.

[47] Y. Kong, D. Yu, B. Zhang, W. Fang, S. Feng, Ultraviolet-emitting ZnO nanowires synthesized by a physical vapor deposition approach, Applied Physics Letters 78 (2001) 407.

[48] T.T. John, K.R. Priolkar, A. Bessi re, P. Sarode, B. Viana, Effect of [OH–] linkages on luminescent properties of ZnO nanoparticles, The Journal of Physical Chemistry C (2011).

[49] M. Baibarac, I. Baltog, T. Velula, I. Pasuk, S. Lefrant, N. Gautier, ZnO particles of wurtzite structure as a component in ZnO/carbon nanotube composite, Journal of Physics: Condensed Matter 21 (2009) 445801.

[50] C. Guillén, J. Herrero, Optical, electrical and structural characteristics of Al: ZnO thin films with various thicknesses deposited by DC sputtering at room temperature and annealed in air or vacuum, Vacuum 84 (7) (2010) 924–929.

[51] S. De, T.M. Higgins, P.E. Lyons, E.M. Doherty, P.N. Nirmalraj, W.J. Blau, J.J. Boland, J.N. Coleman, Silver nanowire networks as flexible, transparent, conducting films: extremely high dc to optical conductivity ratios, ACS Nano 3 (7) (2009) 1767–1774.

[52] S. De, J.N. Coleman, Are there fundamental limitations on the sheet resistance and transmittance of thin graphene films?, ACS Nano 4 (5) (2010) 2713–2720

[53] J. Wu, M. Agrawal, H.A. Becerril, Z. Bao, Z. Liu, Y. Chen, P. Peumans, Organic light-emitting diodes on solution-processed graphene transparent electrodes, ACS Nano 4 (1) (2009) 43–48.

[54] M. Vosgueritchian, D.J. Lipomi, Z. Bao, Highly conductive and transparent PEDOT: PSS films with a fluorosurfactant for stretchable and flexible transparent electrodes, Advanced Functional Materials (2012).